Available online at www.sciencedirect.com
ScienceDirect
*Mendeleev Commun.*, 2015, **25**, 372–374
Mendeleev Communications

# Synthesis and optical properties of oleic-capped CdSe quantum dots doped with silver and indium

**Pavel A. Kotin,* Sergei S. Bubenov, Tatyana A. Kuznetsova and Sergey G. Dorofeev**

*Department of Chemistry, M. V. Lomonosov Moscow State University, 119991 Moscow, Russian Federation. Fax: +7 495 939 0998; e-mail: kotin-pa@mail.ru, dorofeev@inorg.chem.msu.ru*

DOI: 10.1016/j.mencom.2015.09.019

**The stabilizing effect of indium on (Ag,In) doped CdSe quantum dots and the influence of the Ag precursor $Ag_4Cl_4(PPh_3)_4$ on morphology have been revealed.**

Interest in nanomaterials is associated with a quantum-size effect that gives new properties different from those of bulk materials.[1] Colloidal quantum dots are zero-dimensional objects, their properties have been intensively studied after a convenient method of synthesis was offered.[2] After exhaustive investigation into the synthesis for I–VII, II–VI, III–V and IV systems,[1,3] new ways of tuning properties of nanocrystals (surface-modification,[4] modification of shape[5] and doping[6]) are searched. Publication topics in this field vary by both the nature of impurities incorporated into quantum dots (valence, size) and methods of such incorporation (cation exchange method,[7] oleate method[8] and three-part core-shell synthesis[9]). Doping may strongly influence the electrical, magnetic and optical properties of nanocrystals.

Indium is a heterovalent impurity for cadmium selenide. Introduction of In leads to n-type conductivity, as it was observed for Ga-doped CdSe nanowires.[10] Experimental data on the indium location are differing. It was assumed that the greater part of In is located on the surface of nanocrystals. That was confirmed by ligand exchange to pyridine.[11] However, the chemical etching data showed that In uniformly distributed over the entire volume of quantum dots. Such a distribution is explained by the low ability of indium to diffuse through nanocrystals.[9] It was found that the absorption, photoluminescence and structure of In-doped CdSe are similar to those of undoped CdSe nanoparticles.[11] Comparison of theory and experimental data suggests that approximate location of the indium dopant level is at 280 meV below the conduction band edge, electron may fall down on that unoccupied level and the probability of that event depends on temperature.[12]

Incorporation of Ag leads to p-type conductivity (compared to In). There are two methods to incorporate Ag into CdSe quantum dots. The first is cation exchange, which provides high degrees of exchange, often resulting in formation of multiphase nanocrystals or silver chalcogenide nanocrystals due to extreme thermodynamic efficiency of this process and high diffusivity of silver ions.[7] Ag impurities are capable of migration inside the cadmium chalcogenide lattice and are likely to form domains at high enough concentrations. The replacement of CdSe with $Ag_2Se$ results in $< 1\%$ change in unit cell volume.[14] Doping CdSe nanocrystals with silver through cation exchange does not notably affect crystallinity, UV-VIS absorption spectra or size distribution.[15]

Photoluminescence (PL) studies of Ag-doped CdSe quantum dots indicate the emergence of dopant-related size-dependant feature in the long-wavelength part of PL spectra, which was supposed to be caused by recombination of photoexcited electrons with Ag-bound holes. Thus, silver serves like a p-type dopant at higher concentration. At a low doping level, silver just provides a positively charged centre, being an n-type dopant. The addition of 1–2 of silver impurity per nanocrystal strongly improves the quantum yield of luminescence.[14]

The second method to incorporate Ag into CdSe quantum dots is oleic synthesis (the *in situ* doping of CdSe nanocrystals with silver during the colloidal synthesis).[15] X-ray diffraction shows that the only crystalline phase in samples is CdSe. The UV-VIS absorption spectra of the samples are similar to those of undoped CdSe quantum dots.

Here, we propose a modified oleate method (the *in situ* colloidal synthesis) to prepare indium and silver doped CdSe nanocrystals† using a published technique.[15]

Oleate method allowed us to obtain Cd(In,Ag)Se nanocrystals with a maximum Ag-doping level of 0.49% (1.0 Ag atoms per nanocrystal) and In-doping level of 32% (66 In atoms per nanocrystal) (Table 1). Excessive silver precipitated during synthesis

† Indium oleate $In(Ole)_3$ was used as an indium precursor and the complex $Ag_4Cl_4(PPh_3)_4$ as a precursor of silver. The source of cadmium was cadmium oleate prepared beforehand from cadmium acetate and oleic acid dissolved in diphenyl ether. The selenium precursor was a 1 M solution of trioctylphosphine selenide (TOPSe) in trioctylphosphine (TOP) prepared by dissolving selenium powder in TOP. The typical synthetic process was as follows: cadmium precursor solution containing 0.5 mmol of Cd was put in a reactor flask with corresponding amounts of precursors: $Ag_4Cl_4(PPh_3)_4$ (synthesized as described[16]) and $In(Ole)_3$ (synthesized using indium acetate and oleic acid) in 2 ml of diphenyl ether (Table 1). Complex of silver gives a turbid solution with diphenyl ether; thus, two drops of TOP were added to obtain a clear solution. Next, the mixture was heated to 200 or 220 °C (Table 1) in Ar and 0.45 ml of a 1 M TOPSe solution in TOP were injected with stirring. After particle growth for 5 min, the reaction system was cooled to room temperature. Typically, 5–20 s after injection, the solution changed from pale yellow to yellow and then to red. The post-synthetic treatment of samples included iterative additions of acetone as a coagulant, resulting in the precipitation of quantum dots, and dissolving them in hexane. This was done to remove organic impurities and by-products. The samples were stored in glass vials, dissolved in hexane.

The elemental analysis was performed with a Bruker M1 Mistral μ-XRF spectrometer. The Ag-to-Cd and In-to-Cd ratios were determined from the relative intensity of Kα peaks using a calibration curve. The UV-VIS absorption was studied with a Varian Cary 50 spectrophotometer from 300 to 1000 nm. The fluorescence measurements were done with a 405 nm laser and detected by an Ocean Optics 4000 USB spectrometer calibrated by 2600 K W-lamp (450–1100 nm). The energy quantum yields were determined in diluted sols relative to a Rhodamine 6G solution of the same absorbance at 405 nm. Transmission electron microscopy (TEM) was performed on a LEO912 AB OMEGA microscope with an accelerating voltage of 200 kV. Size distributions were obtained through manual calculations of quantum dots images.

**Table 1** Synthetic conditions and select parameters of synthesized nanocrystals.

| | $T_{synth}$/°C | Cd:In:Ag ratio | In to Cd in nanocrystals (%) | In atoms per nanocrystal | Ag to Cd in nanocrystals (%) | Ag atoms per nanocrystal | Diameter/nm |
|---|---|---|---|---|---|---|---|
| Sample 1 | 200 | 10:4:0.5 | 2.8±0.4 | 8.6 | 0.27±0.05 | 0.82 | 3.2 |
| Sample 2 | 200 | 10:4:2 | 2.2±0.4 | 6.8 | 0.17±0.05 | 0.52 | 3.2 |
| Sample 3 | 200 | 10:4:4 | 32±2 | 66 | 0.49±0.05 | 1.0 | 2.8 |
| Sample 4 (tetrapods) | 200 | 10:4:10 | 4.6±0.4 | 15 (in tp leg) | 0.21±0.05 | 0.7 (in tp leg) | Length 5.5, width 2.3 |
| Sample 5 | 220 | 10:4:0 | 8.7±0.5 | 35 | — | — | 3.5 |

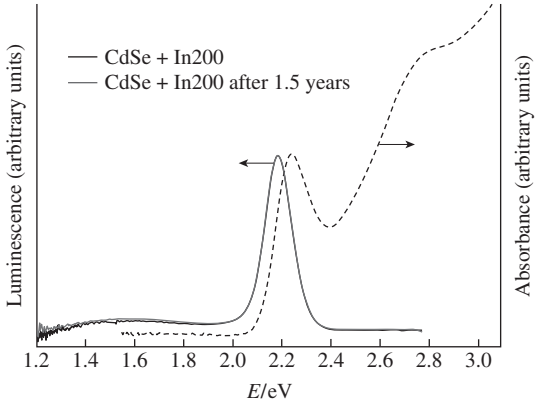


**Figure 1** PL and UV-VIS absorption spectra of sample 5.

as $Ag_2Se$; therefore, the Ag to Cd ratio in Cd(In,Ag)Se quantum dots is low.

The PL of In-doped quantum dots was similar to that of undoped nanocrystals (Figure 1),[11] but the simultaneous addition of Ag and In precursors caused a long wavelength feature to appear near the band-edge peak, which will be later referred to as the A-band. The form of spectra for samples 1–4 also changed over time (Figure 2), with A-band intensity rising *versus* the band-edge peak. Quantum yield has increased during this alteration, and it probably means that impurities were redistributed inside the nanoparticles. The PL spectra acquired for the samples with simultaneous doping have a shape similar to that of samples synthesized without In precursor; however, simultaneous doping slows down the aging of the nanocrystals (in comparison to Ag-doped).

The surface of nanocrystals is active due to the presence of dangling bonds. Cadmium can fulfill its valent potential by connecting with oleic acid, whereas selenium bonds on the surface are not saturated. That circumstance caused exciton traps to appear on the surface, leading to reduction of the quantum yield. We assumed that immediately after the synthesis impurities are uniformly distributed in nanocrystals. Silver brings a considerable amount of defects to the structure that causes the increase in A-band intensity in PL spectra. Exclusion of silver from the volume to the surface of the nanocrystals is accompanied by an increase in the amount of volume defects, but the termination of surface selenium bounds ultimately leads to an overall increase in quantum yield. High-level doping results in emergence of a strongly defect structure in low quantum yield. That feature was described previously:[14] at low doping levels, quantum yield exceeded that of undoped nanocrystals and at high doping levels quantum yield was lower than that of undoped quantum dots.

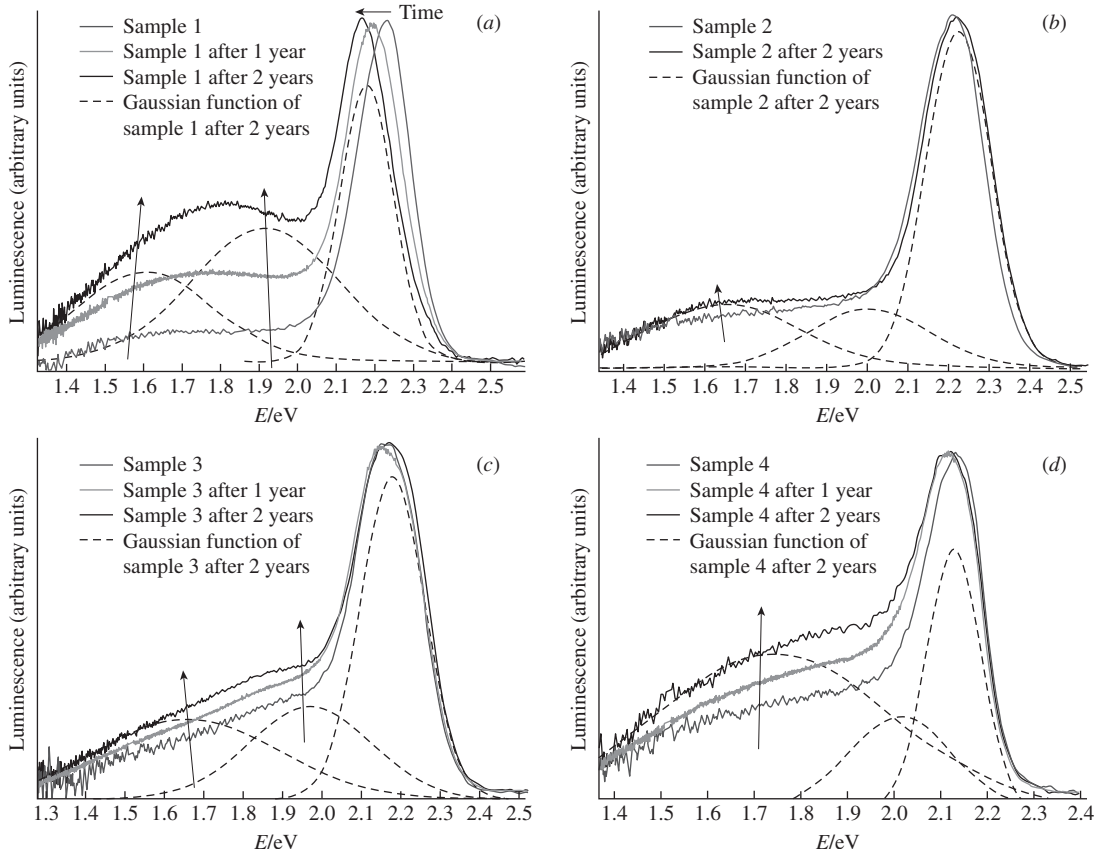


**Figure 2** PL spectra of samples (*a*) 1, (*b*) 2, (*c*) 3 and (*d*) 4.

Incorporation of silver simultaneously with indium should enhance the stability of nanocrystals because the sum of ionic radii of indium and silver is close to the doubled ionic radius of cadmium. It was not observed for the incorporation of silver impurities only.[15] The replacement of two cadmium ions in a nanocrystal lattice by indium and silver also should compensate differences in Cd, In, and Ag charges and decrease the number of vacancies in quantum dots.

$r(Cd^{2+}) + r(Cd^{2+}) = 0.95$ Å + 0.95 Å = 1.90 Å (for coordination VI)

$r(In^{3+}) + r(Ag^{+}) = 0.8$ Å + 1.15 Å = 1.95Å (for coordination VI)[17,18]

Indeed, simultaneous In/Ag doping slows down the aging of nanocrystals (rate of alteration of PL spectra) (Figure 2). Average lifetime of quantum dot samples is dramatically increased (compared to Ag-doped CdSe quantum dots[15]). The driving force behind the process of aging of the nanoparticles is likely to be the expulsion of silver atoms. This phenomenon of the so-called self-purification is well known and results from thermodynamic preference to expel dopants from the structure of the NPs to minimize the overall free energy.[19,20]

Unit-cell parameters for sample 3 were found from XRD analysis and were similar to those of undoped nanocrystals of CdSe (Figure S1, Online Supplementary Materials). However, it does not exclude the possibility of formation of CdSe–$In_2Se_3$ solid solution because the volume attributable to 1 atom in the structures of CdSe and $In_2Se_3$ is almost the same, 28.05 and 28.43 Å$^3$, respectively (PC-PDF ICDD C8-459 and C40-1407 cards). Thus, the replacement of Cd ions by In causes one vacancy to appear (as in $In_2Se_3$), and cell parameters remain almost unchanged. Since metal vacancies give levels in CdSe bang gap, the introduction of a lot of metal vacancies should lead to a decrease in quantum yield and, probably, to the appearance of a new non-excitonic low-energy PL. We did not observe any decrease in quantum yield or emergence of a new low-energy luminescence (see IR-VIS PL spectrum of sample 3 in Figure S2, Online Supplementary Materials). It indirectly confirms that amount of indium into nanocrystals did not exceed the amount of dissolved silver and that indium is mostly located on the surface of nanocrystals.

It is interesting that nanocrystals change their shape from sphere to oblong structures when the number of Ag precursors in synthesis is increased (Figure 3). Sample 1 [Figure 3(*a*)] contains only spherical particles with an average diameter of 3 nm (FWHM 2 nm). In sample 2, ellipsoidal particles are found and the amount of these particles is increased in sample 3 [Figure 3(*b*),(*c*)]; nevertheless, the average diameter of the nanocrystals is 3 nm (FWHM 1 and 2 nm). Sample 4 almost completely consists of oblong and branched structures [Figure 3(*d*)], the average diameter and length of legs are 2.3 nm (FWHM 1 nm) and 5.5 nm (FWHM 3 nm), respectively. We associate the growth of anisotropic particles in case of sample 4 with the presence of chloride ions in silver precursor. Tetrapod particles were successively obtained[21] from nuclei of zincblende structure through the addition of organic precursors of halide ions.

Thus, the optical properties, structure and shape of quantum dots doped only with indium are similar to those of undoped nanocrystals. Simultaneous In/Ag-doping slows down the aging of nanocrystals (as compared with Ag-doped ones). The increase in amount of Ag-precursor in synthesis leads to the formation of oblong structures.

This work was supported by the Russian Foundation for Basic Research (project no. 12-03-00933 a).

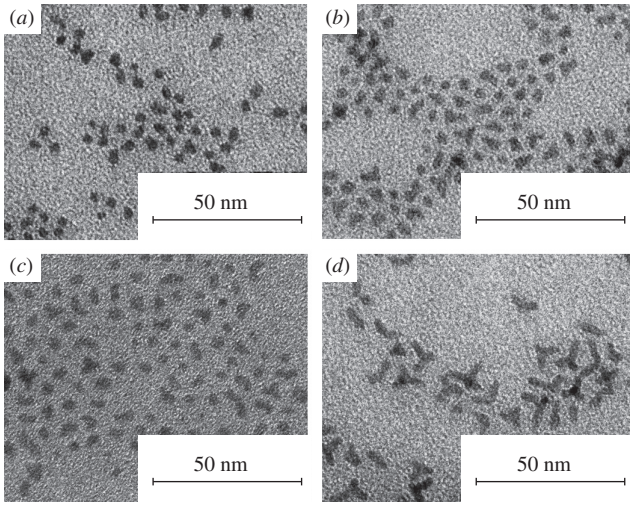


**Figure 3** TEM images of samples (*a*) 1, (*b*) 2, (*c*) 3 and (*d*) 4.

*Online Supplementary Materials*

Supplementary data associated with this article can be found in the online version at doi:10.1016/j.mencom.2015.09.019.

## References

1 O. I. Micic, H. M. Cheong, H. Fu, A. Zunger, J. R. Sprague, A. Mascarenhas and A. J. Nozik, *J. Phys. Chem. B*, 1997, **101**, 4904.
2 C. B. Murray, D. J. Norris and M. G. Bawendi, *J. Am. Chem. Soc*., 1993, **115**, 8706.
3 E. Lifshitz, A. Glozman, I. D. Litvin and H. Porteanu, *J. Phys. Chem. B*, 2000, **104**, 10449.
4 D. A. Hines and P. V. Kamat, *ACS Appl. Mater. Interfaces*, 2014, **6**, 3041.
5 H. Shen, H. Wang, X. Chen, J. Z. Niu, W. Xu, X. M. Li, X.-D. Jiang, Z. Du and L. S. Li, *Chem. Mater.*, 2010, **22**, 4756.
6 D. J. Norris, A. L. Efros and S. C. Erwin, *Science*, 2008, **319**, 1776.
7 D. H. Son, S. M. Hughes, Y. Yin and A. P. Alivisatos, *Science*, 2004, **306**, 1009.
8 P. N. Tananaev, S. G. Dorofeev, R. B. Vasil'ev and T. A. Kuznetsova, *Inorg. Mater.*, 2009, **45**, 347 (*Neorg. Mater.*, 2009, **45**, 393).
9 A. W. Wills, M. S. Kang, K. M. Wentz, S. E. Hayes, A. Sahu, W. L. Gladfelter and D. J. Norris, *J. Mater. Chem*., 2012, **22**, 6335.
10 Z. Hu, X. Zhang, C. Xie, C. Wu, X. Zhang, L. Bian, Y. Wu, L. Wang, Y. Zhang and J. Jie, *Nanoscale*, 2011, **3**, 4798.
11 C. K. Knox, S. D. Fillmore, D. M. Call, D. G. Allen, B. C. Hess, R. C. Davis, W. E. Evenson and R. G. Harrison, *J. Colloid Interface Sci*., 2006, **300**, 591.
12 S. Roy, C. Tuinenga, F. Fungura, P. Dagtepe and V. Chikan, *J. Phys. Chem. C*, 2009, **113**, 13008.
13 B. J. Beberwyck, Y. Surendranath and A. P. Alivisatos, *J. Phys. Chem. C*, 2013, **117**, 19759.
14 A. Sahu, M. S. Kang, A. Kompch, C. Notthoff, A. W. Wills, D. Deng, M. Winterer, C. D. Frisbie and D. J. Norris, *Nano Lett*., 2012, **12**, 2587.
15 S. S. Bubenov, S. G. Dorofeev, P. A. Kotin, K. O. Znamenkov and T. A. Kuznetsova, *Mendeleev Commun*., 2014, **24**, 250.
16 B.-K. Teo and J. C. Calabrese, *Inorg. Chem.*, 1976, **15**, 2467.
17 R. D. Shannon, *Acta Crystallogr.*, 1976, **A32**, 751.
18 L. Pauling, T*he Nature of the Chemical Bond*, 3rd edn., Cornell University Press, Ithaca, NY, 1960.
19 S. C. Erwin, L. Zu, M. I. Haftel, A. L. Efros, T. A. Kennedy and D. J. Norris, *Nature*, 2005, **436**, 91.
20 G. M. Dalpian and J. R. Chelikowsky, *Phys. Rev. Lett.*, 2006, **96**, 226802.
21 J. Lim, W. K. Bae, K. U. Park, L. zur Borg, R. Zentel, S. Lee and K. Char, *Chem. Mater*., 2013, **25**, 1443.

*Received: 12th February 2015; Com. 15/4563*